

ASME-ATI-
UIT 2010,
Sorrento,
Italy

J.I. Ramos
and Francisco
J. Blanco-
Rodríguez

Introduction

Mathematical
formulation

Numerical
method

Numerical
results

Two-
dimensional
model numerical
results

Comparison
with
one-dimensional
model

Conclusions

MODELLING OF MOLECULAR ORIENTATION AND CRYSTALLIZATION IN THE MANUFACTURE OF SEMI-CRYSTALLINE COMPOUND FIBRES

J.I. Ramos and **Francisco J. Blanco-Rodríguez**

Escuela de Ingenierías
Universidad de Málaga, Spain

Conference on Thermal and Environmental Issues in
Energy Systems
16–19 May 2010, Sorrento, Italy

ASME-ATI-
UIT 2010,
Sorrento,
Italy

J.I. Ramos
and Francisco
J. Blanco-
Rodríguez

Introduction

Mathematical
formulation

Numerical
method

Numerical
results

Two-
dimensional
model numerical
results

Comparison
with
one-dimensional
model

Conclusions

- 1 Introduction
- 2 Mathematical formulation
- 3 Numerical method
- 4 Numerical results
 - Two-dimensional model numerical results
 - Comparison with one-dimensional model
- 5 Conclusions

ASME-ATI-UIT 2010,
Sorrento,
Italy

J.I. Ramos
and Francisco
J. Blanco-
Rodríguez

Introduction

Mathematical
formulation

Numerical
method

Numerical
results

Two-
dimensional
model numerical
results

Comparison
with
one-dimensional
model

Conclusions

- Bi-component compound fibres are manufactured by MELT SPINNING processes.
- Applications
 - 1 Telecommunications: Data transmission.
 - 2 Chemical industry: Filtration and separation processes.
 - 3 Biomedical industry.
 - 4 Textile industry.
- Necessary: modelling of the drawing process for both hollow and solid semi-crystalline compound fibres.
- Previous studies are based on one-dimensional models of amorphous, slender fibres at low Re .
- NO INFORMATION ABOUT RADIAL VARIATIONS.
- Use of a hybrid model for fibre spinning.

ASME-ATI-UIT 2010,
Sorrento,
Italy

J.I. Ramos
and Francisco
J. Blanco-Rodríguez

Introduction

Mathematical
formulation

Numerical
method

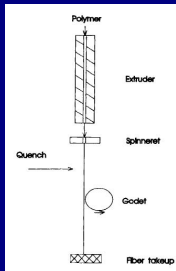
Numerical
results

Two-
dimensional
model numerical
results

Comparison
with
one-dimensional
model

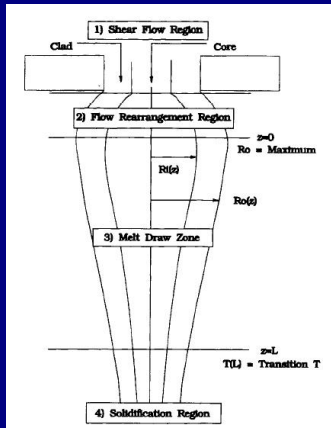
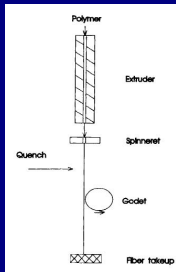
Conclusions

Involves the extrusion and drawing of a polymer cylinder. Four zones.



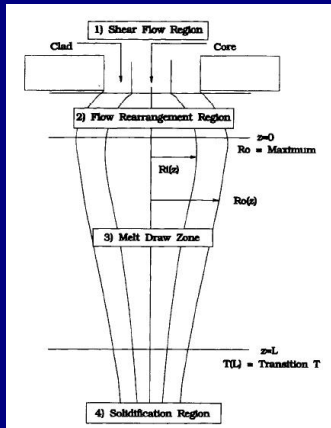
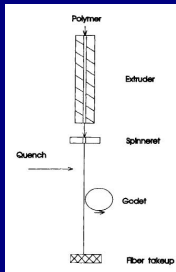
- ① Shear Flow Region.
- ② Flow Rearrangement Region.
- ③ Melt Drawing Zone.
- ④ Solidification region.

Involves the extrusion and drawing of a polymer cylinder. Four zones.



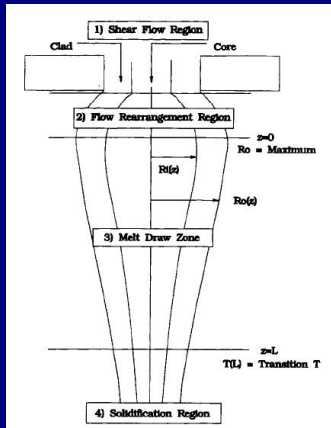
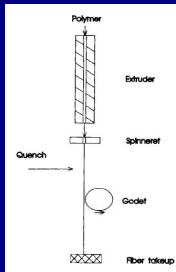
- ① Shear Flow Region.
- ② Flow Rearrangement Region.
- ③ Melt Drawing Zone.
- ④ Solidification region.

Involves the extrusion and drawing of a polymer cylinder. Four zones.



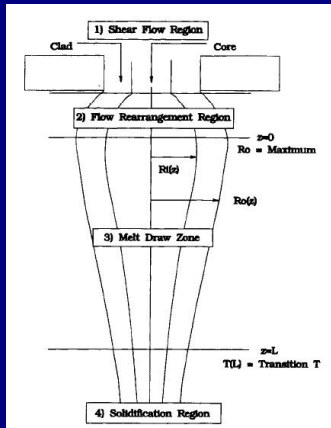
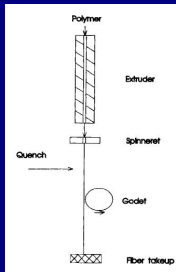
- 1 Shear Flow Region.
- 2 Flow Rearrangement Region.
- 3 Melt Drawing Zone.
- 4 Solidification region.

Involves the extrusion and drawing of a polymer cylinder. Four zones.



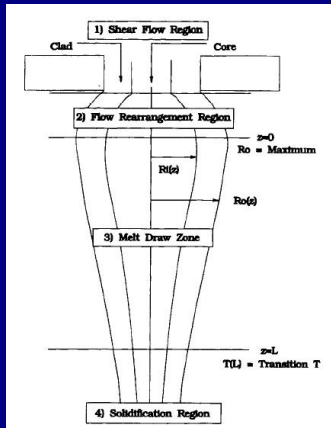
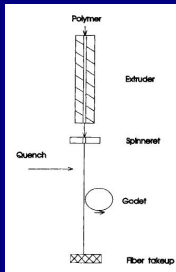
- 1 Shear Flow Region.
- 2 Flow Rearrangement Region.
- 3 Melt Drawing Zone.
- 4 Solidification region.

Involves the extrusion and drawing of a polymer cylinder. Four zones.



- 1 Shear Flow Region.
- 2 Flow Rearrangement Region.
- 3 **Melt Drawing Zone.**
- 4 Solidification region.

Involves the extrusion and drawing of a polymer cylinder. Four zones.



- 1 Shear Flow Region.
- 2 Flow Rearrangement Region.
- 3 Melt Drawing Zone.
- 4 Solidification region.

Mathematical formulation (I)

ASME-ATI-UIT 2010,
Sorrento,
Italy

J.I. Ramos
and Francisco
J. Blanco-
Rodríguez

Introduction

Mathematical
formulation

Numerical
method

Numerical
results

Two-
dimensional
model numerical
results
Comparison
with
one-dimensional
model

Conclusions

- Mass conservation equation

$$\nabla \cdot \mathbf{v}_i = 0 \quad i = 1, 2,$$

where $\mathbf{v} = u(r, x) \mathbf{e}_x + v(r, x) \mathbf{e}_r$

- Linear Momentum conservation equation

$$\rho_i \left(\frac{\partial \mathbf{v}_i}{\partial t} + \mathbf{v}_i \cdot \nabla \mathbf{v}_i \right) = -\nabla p + \nabla \cdot \boldsymbol{\tau}_i + \rho_i \cdot \mathbf{f}^m \quad i = 1, 2,$$

where $\mathbf{f}^m = g \mathbf{e}_x$

- Energy conservation equation

$$\rho_i C_i \left(\frac{\partial T_i}{\partial t} + \mathbf{v}_i \cdot \nabla T_i \right) = -k_i \Delta T_i \quad i = 1, 2,$$

- Constitutive equations

- Rheology

$$\boldsymbol{\tau} = \mu_{eff} (\nabla \mathbf{v} + \nabla \mathbf{v}^T) + \boldsymbol{\tau}_p,$$

where

$$\boldsymbol{\tau}_p = 3c k_B T \left[-\frac{\lambda}{\phi} F(\mathbf{S}) + 2\lambda (\nabla \mathbf{v}^T : \mathbf{S}) (\mathbf{S} + \mathbf{I}/3) \right]$$

ASME-ATI-UIT 2010,
Sorrento,
Italy

J.I. Ramos
and Francisco
J. Blanco-Rodríguez

Introduction

Mathematical
formulation

Numerical
method

Numerical
results

Two-
dimensional
model numerical
results

Comparison
with
one-dimensional
model

Conclusions

- **Molecular orientation tensor equation: Doi–Edwards theory**

$$\mathbf{S}_{(1)} = F(\mathbf{S}) + G(\nabla \mathbf{v}, \mathbf{S}),$$

$$F(\mathbf{S}) = -\frac{\phi}{\lambda} \{ (1 - N/3) \mathbf{S} - N (\mathbf{S} \cdot \mathbf{S}) + N (\mathbf{S} : \mathbf{S}) (\mathbf{S} + \mathbf{I}/3) \}$$

$$G(\nabla \mathbf{v}, \mathbf{S}) = \frac{1}{3} (\nabla \mathbf{v} + \nabla \mathbf{v}^T) - 2 (\nabla \mathbf{v}^T : \mathbf{S}) (\mathbf{S} + \mathbf{I}/3).$$

where subscript (1) denote UCTD operator

$$\Lambda_{(1)} = \frac{\partial \Lambda}{\partial t} + \mathbf{v} \cdot \nabla \Lambda - (\nabla \mathbf{v}^T \cdot \Lambda + \Lambda \cdot \nabla \mathbf{v})$$

- **Molecular orientation scalar order parameter**

$$S \equiv \sqrt{\frac{3}{2} (\mathbf{S} : \mathbf{S})} \quad \mathbf{S} = \text{diag} (S_{rr}, S_{\theta\theta}, S_{xx}),$$

- **Crystallization: Avrami–Kolmogorov's theory & Ziabicki's model**

$$\frac{\partial \mathcal{X}_i}{\partial t} + \mathbf{v} \cdot \nabla \mathcal{X}_i = k_{Ai}(\mathcal{S}_i) (\mathcal{X}_{\infty,i} - \mathcal{X}_i) \quad i = 1, 2,$$

where

$$k_{Ai}(\mathcal{S}_i) = k_{Ai}(0) \exp(a_{2i} \mathcal{S}_i^2), \quad i = 1, 2.$$

Mathematical formulation (III)

ASME-ATI-UIT 2010,
Sorrento,
Italy

J.I. Ramos
and Francisco
J. Blanco-
Rodríguez

Introduction

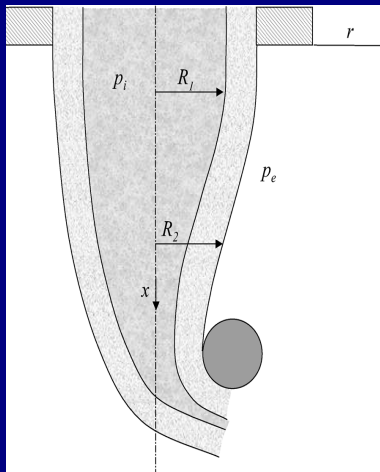
Mathematical
formulation

Numerical
method

Numerical
results

Two-
dimensional
model numerical
results
Comparison
with
one-dimensional
model

Conclusions



Kinematic, dynamic and thermal boundary conditions are required:

- Initial conditions ($t = 0$)
- Symmetry conditions ($r = 0$)
- Die exit conditions ($x = 0$)
- Take-up point conditions ($x = L$)
- Conditions on free surfaces of compound fibre ($r = R_1(x)$ and $r = R_2(x)$)

- Non-dimensional variables

$$\hat{t} = \frac{t}{(L/u_0)} \quad \hat{r} = \frac{r}{R_0} \quad \hat{x} = \frac{x}{L} \quad \Rightarrow \quad \epsilon = \frac{R_0}{L}$$

$$\hat{u} = \frac{u}{u_0} \quad \hat{v} = \frac{v}{(u_0 \epsilon)} \quad \hat{p} = \frac{p}{(\mu_0 u_0 / L)} \quad \hat{T} = \frac{T}{T_0}$$

$$\hat{\rho} = \frac{\rho}{\rho_0} \quad \hat{C} = \frac{C}{C_0} \quad \hat{\mu} = \frac{\mu}{\mu_0} \quad \hat{k} = \frac{k}{k_0}$$

- Non-dimensional numbers

$$Re = \frac{\rho_0 u_0 R_0}{\mu_0}, \quad Fr = \frac{u_0^2}{g R_0}, \quad Ca = \frac{\mu_0 u_0}{\sigma_2},$$

$$Pr = \frac{\mu_0 C_0}{k_0}, \quad Pe = Re Pr, \quad Bi = \frac{h R_0}{k_0}$$

- ASME-ATI-UIT 2010, Sorrento, Italy
- J.I. Ramos and Francisco J. Blanco-Rodríguez
- Introduction
- Mathematical formulation
- Numerical method
- Numerical results
- Two-dimensional model numerical results
- Comparison with one-dimensional model
- Conclusions

- **Asymptotic method using the fibre slenderness, $\epsilon \ll 1$, as perturbation parameter**

$$\Psi_i = \Psi_{i,0} + \epsilon^2 \Psi_{i,2} + O(\epsilon^4),$$

for the variables $\hat{R}_i, \hat{u}_i, \hat{v}_i, \hat{p}_i$ and \hat{T}_i where $i = 1, 2$.

- **Flow regime considered for steady ($\frac{\partial}{\partial t} = 0$) jets**

$$Re = \epsilon \bar{R}, \quad Fr = \frac{\bar{F}}{\epsilon}, \quad Ca = \frac{\bar{C}}{\epsilon},$$

$$Pe = \epsilon \bar{P}, \quad Bi = \epsilon^2 \bar{B}$$

where $\bar{\Upsilon} = O(1)$.

ASME-ATI-UIT 2010,
Sorrento,
Italy

J.I. Ramos
and Francisco
J. Blanco-Rodríguez

- Asymptotic one-dimensional mass conservation equation

$$\mathcal{A}_1 U = Q_1, \quad \mathcal{A}_2 U = Q_2$$

where

$$\mathcal{A}_1 = \frac{\mathcal{R}_1^2}{2}, \quad \mathcal{A}_2 = \frac{\mathcal{R}_2^2 - \mathcal{R}_1^2}{2},$$

- Asymptotic one-dimensional linear momentum equation

$$\begin{aligned} \bar{R}(\hat{\rho}_1 \mathcal{A}_1 + \hat{\rho}_2 \mathcal{A}_2) \mathcal{U} \frac{d\mathcal{U}}{d\hat{x}} &= \frac{d}{d\hat{x}} \left(3 \langle \hat{\mu}_{eff,1} \rangle \mathcal{A}_1 + \langle \hat{\mu}_{eff,2} \rangle \mathcal{A}_2 \right) \frac{d\mathcal{U}}{d\hat{x}} \\ &+ \frac{1}{2\bar{C}} \left(\frac{d\mathcal{R}_2}{d\hat{x}} + \frac{\sigma_1}{\sigma_2} \frac{d\mathcal{R}_1}{d\hat{x}} \right) \\ &+ (\hat{\rho}_1 \mathcal{A}_1 + \hat{\rho}_2 \mathcal{A}_2) \frac{\bar{R}}{\bar{F}} \end{aligned}$$

- Radial velocity field

$$\mathcal{V}(\hat{r}, \hat{x}) = -\frac{\hat{r}}{2} \frac{d\mathcal{U}}{d\hat{x}},$$

Introduction

Mathematical
formulation

Numerical
method

Numerical
results

Two-
dimensional
model numerical
results

Comparison
with
one-dimensional
model

Conclusions

Mapping: 2D model

$(\hat{r}, \hat{x}) \mapsto (\xi, \eta)$ maps $\Omega_{\hat{r}\hat{x}} = \{[0, \mathcal{R}_2(\hat{x})] \times [0, 1]\}$ into a rectangular domain $\Omega_{\xi\eta} = \{[0, 1] \times [0, 1]\}$

ASME-ATI-UIT 2010,
Sorrento,
Italy

J.I. Ramos
and Francisco
J. Blanco-
Rodríguez

Introduction

Mathematical
formulation

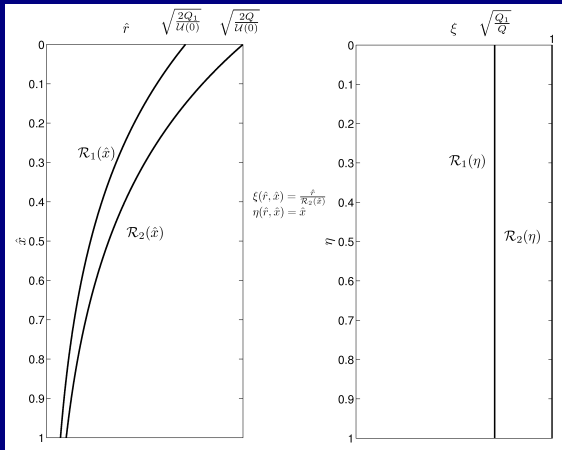
Numerical
method

Numerical
results

Two-
dimensional
model numerical
results

Comparison
with
one-dimensional
model

Conclusions



- Two-dimensional energy equation

$$\frac{\partial \hat{T}_i}{\partial \eta} = \frac{1}{2Q} \frac{1}{\bar{P}_i} \frac{1}{\xi} \frac{\partial}{\partial \xi} \left(\xi \frac{\partial \hat{T}_i}{\partial \xi} \right) \quad i = 1, 2,$$

- Two-dimensional degree of crystallinity equation

$$\hat{U} \frac{\partial \mathcal{X}_i}{\partial \eta} = k_{Ai}(0) \exp(a_{2i} \mathcal{S}_i^2) (\mathcal{X}_{\infty,i} - \mathcal{X}_i), \quad i = 1, 2,$$

- Effective dynamic viscosity

$$\hat{\mu}_{eff,i} = \hat{G}_i \exp \left(\hat{E}_i (1 - \hat{T}_i) + \beta_i \left(\frac{\mathcal{X}_i}{\mathcal{X}_{\infty,i}} \right)^{n_i} \right) \quad i = 1, 2.$$

ASME-ATI-UIT 2010,
Sorrento,
Italy

J.I. Ramos
and Francisco
J. Blanco-
Rodríguez

Introduction

Mathematical
formulation

Numerical
method

Numerical
results

Two-
dimensional
model numerical
results
Comparison
with
one-dimensional
model

Conclusions

$$U \frac{\partial S_{i rr}}{\partial \eta} = \left(S_{i rr} + \frac{1}{3} \right) (S_{i rr} + S_{i \theta \theta} + S_{i x x} - 1) \frac{dU}{d\eta}$$

$$- \frac{\phi}{\lambda} \left\{ S_{i rr} - N \left[\left(S_{i rr} + \frac{1}{3} \right) (S_{i rr} - \Pi_{i s}) \right] \right\}, \quad i = 1, 2,$$

$$U \frac{\partial S_{i \theta \theta}}{\partial \eta} = \left(S_{i \theta \theta} + \frac{1}{3} \right) (S_{i rr} + S_{i \theta \theta} + S_{i x x} - 1) \frac{dU}{d\eta}$$

$$- \frac{\phi}{\lambda} \left\{ S_{i \theta \theta} - N \left[\left(S_{i \theta \theta} + \frac{1}{3} \right) (S_{i \theta \theta} - \Pi_{i s}) \right] \right\}, \quad i = 1, 2,$$

$$U \frac{\partial S_{i x x}}{\partial \eta} = \left(S_{i x x} + \frac{1}{3} \right) (S_{i rr} + S_{i \theta \theta} + S_{i x x} + 2) \frac{dU}{d\eta}$$

$$- \frac{\phi}{\lambda} \left\{ S_{i x x} - N \left[\left(S_{i x x} + \frac{1}{3} \right) (S_{i x x} - \Pi_{i s}) \right] \right\}, \quad i = 1, 2,$$

$$\Pi_{i s} = S_{i rr}^2 + S_{i \theta \theta}^2 + S_{i x x}^2.$$

Two-dimensional velocity field ($\bar{B} = 5$)

ASME-ATI-UIT 2010,
Sorrento,
Italy

J.I. Ramos
and Francisco
J. Blanco-
Rodríguez

Introduction

Mathematical
formulation

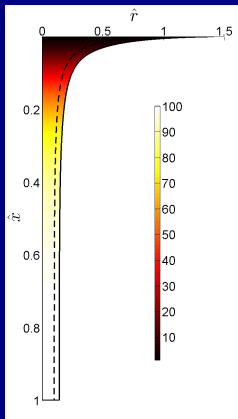
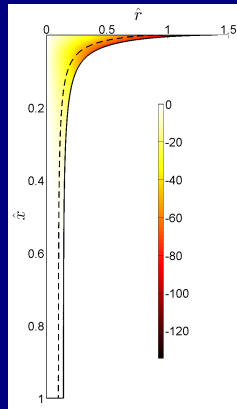
Numerical
method

Numerical
results

Two-
dimensional
model numerical
results

Comparison
with
one-dimensional
model

Conclusions


 $U(\hat{r}, \hat{z})$

 $V(\hat{r}, \hat{z})$

Influence of Biot number on cooling process

ASME-ATI-UIT 2010,
Sorrento,
Italy

J.I. Ramos
and Francisco
J. Blanco-Rodríguez

Introduction

Mathematical
formulation

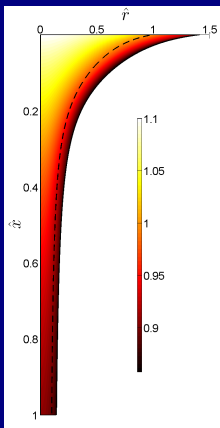
Numerical
method

Numerical
results

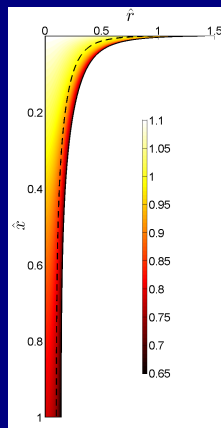
Two-
dimensional
model numerical
results

Comparison
with
one-dimensional
model

Conclusions



$$\bar{B} = 1$$



$$\bar{B} = 5$$

Analysis of the 2D model

ASME-ATI-UIT 2010,
Sorrento,
Italy

J.I. Ramos
and Francisco
J. Blanco-Rodríguez

Introduction

Mathematical
formulation

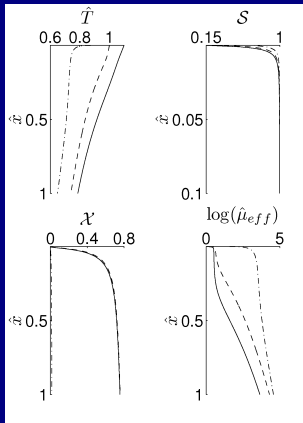
Numerical
method

Numerical
results

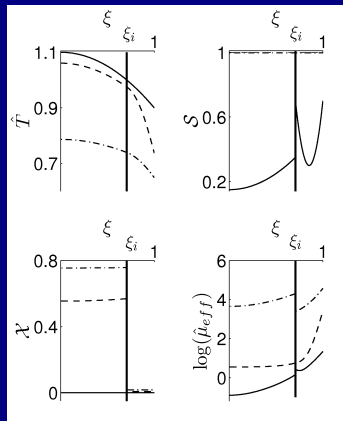
Two-
dimensional
model numerical
results

Comparison
with
one-dimensional
model

Conclusions



$\hat{r} = 0$ (-), $\hat{r} = \mathcal{R}_1^-$ (- -) and $\hat{r} = \mathcal{R}_2$ (- · -)



$\eta = 0$ (-), $\eta = 0,1$ (- -) and $\eta = 1$ (- · -)

ASME-ATI-UIT 2010,
Sorrento,
Italy

J.I. Ramos
and Francisco
J. Blanco-
Rodríguez

Introduction

Mathematical
formulation

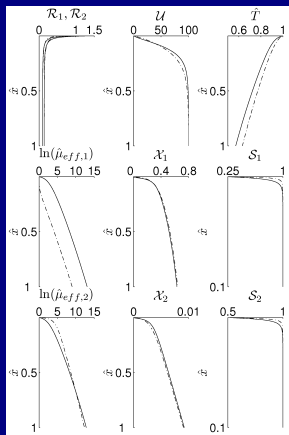
Numerical
method

Numerical
results

Two-
dimensional
model numerical
results

Comparison
with
one-dimensional
model

Conclusions



1D (—) and 2D (---)

ASME-ATI-UIT 2010,
Sorrento,
Italy

J.I. Ramos
and Francisco
J. Blanco-
Rodríguez

Introduction

Mathematical
formulation

Numerical
method

Numerical
results

Two-
dimensional
model numerical
results

Comparison
with
one-dimensional
model

Conclusions

Contributions of the present work:

- 1 Development of a $1 + 1/2D$ model for both amorphous and semicrystalline fibres with modified Newtonian rheology.
- 2 Validation of applicability range of the 1D model with the $1 + 1/2D$ one for slender fibres.
- 3 Determination of the two-dimensional fields of temperature, molecular orientation tensor and degree of crystallinity for solid compound fibres.
- 4 Find substantial temperature non-uniformities (affect the degree of crystallization and have great effects on the properties of compound fibres) in the radial direction exist even at small Biot numbers.

ASME-ATI-UIT 2010,
Sorrento,
Italy

J.I. Ramos
and Francisco
J. Blanco-
Rodríguez

Francisco J. Blanco-Rodríguez

e-mail: fjblanco@lcc.uma.es

website: <http://www.lcc.uma.es/~fjblanco>

J. I. Ramos

e-mail: jirs@lcc.uma.es

Document created by \LaTeX (Beamer class).

**THANK YOU FOR YOUR
ATTENTION**

Introduction

Mathematical
formulation

Numerical
method

Numerical
results

Two-
dimensional
model numerical
results

Comparison
with
one-dimensional
model

Conclusions